Supplement

Table S1: Emission limits set by the CCNR (CCNR, 2022) and the EU (European Union, 2016) in comparison with mean emission factors from this study (measured at BRI).

Emission standard	Valid from year	NO_x limit (g kWh^{-1})	E_{NOx} (this study)	PM limit (g kWh^{-1})	E_{PM} (this study)	PNC limit (10^{12} particles kWh^{-1})
none	≤ 2003	none		none		none
CCNR I	> 2003	9.2	8.9 ± 3.2	0.54	0.35 ± 0.21	none
CCNR II	> 2007	6	8.7 ± 3.2	0.2	0.41 ± 0.20	none
Euro IIIa	> 2007	6	7.0 ± 2.5	0.2	0.44 ± 0.28	none
Euro V[a]	> 2020		0.6 ± 0.5		0.01 ± 0.02	
IWP/IWA		1.8		0.015		1
NRE, P<560kW		0.4		0.015		1
Euro VI marinized		0.4		0.01		0.8

[a]Subcategories according to EU 2016/1628: IWP/IWA = motors certified for inland ships. NRE = motors for non-road mobile machines. Marinized = marinized motors from heavy-duty vehicles.

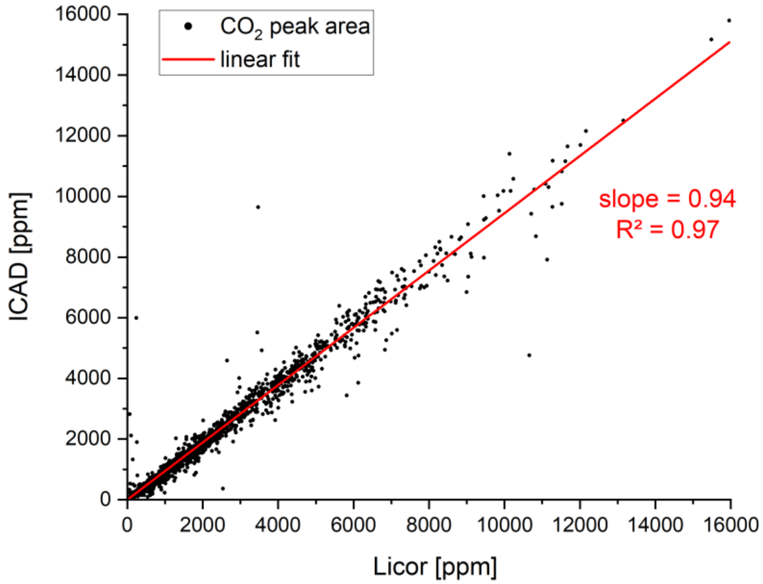

Figure S1: Correlation plot of CO_2 peak areas derived from Licor and ICAD measurements at BRI.

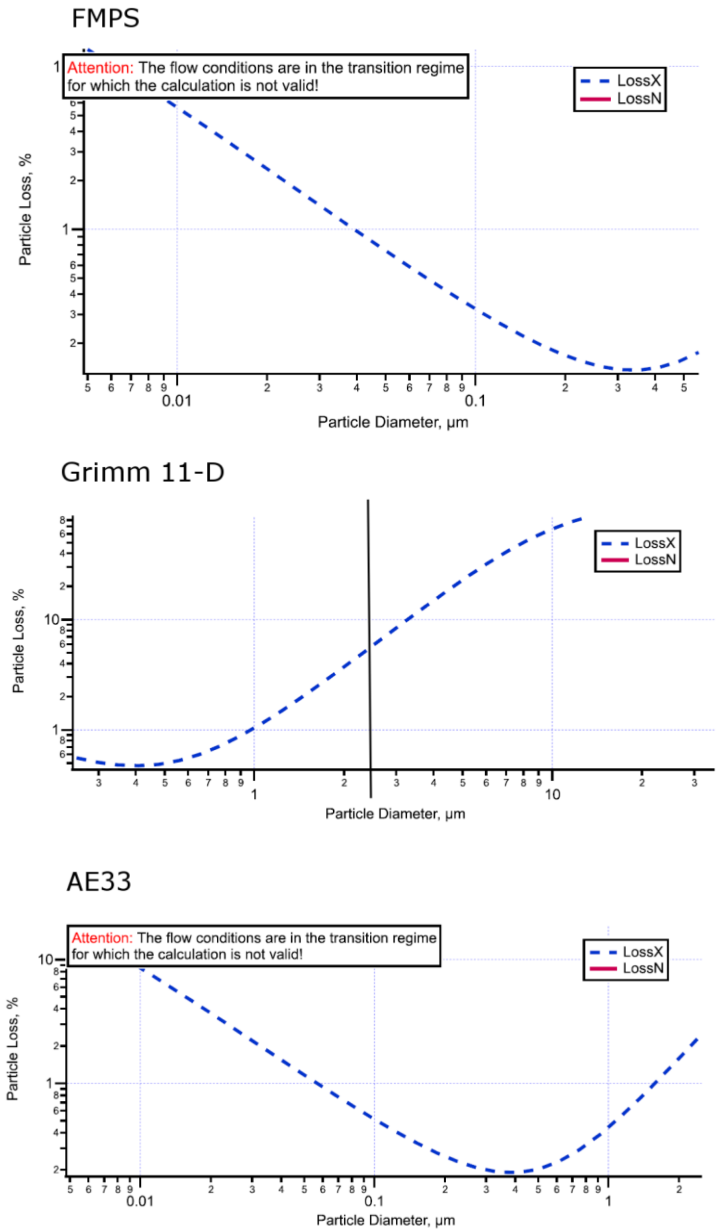

Figure S2: Calculated overall transmission losses for the instruments FMPS, Grimm 11-D and AE33, derived using the Particle Loss Calculator Tool (von der Weiden et al., 2009). To carry out calculations in the transition regime between laminar and turbulent flow (2000<Re<4000) laminar equations were extended to this regime. The results marked with an info box have a lower precision but still provide useful estimates of occurring losses.

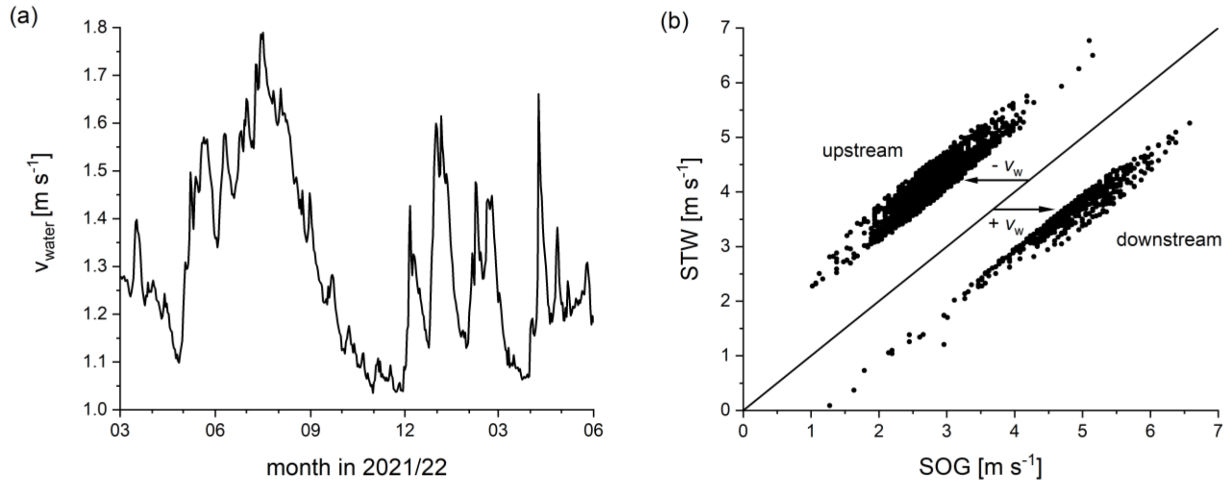

Figure S3: (a) Evolution of the velocity of the Rhine (v_{water}) within the measurement period. (b) Comparison of SOG and STW for ships travelling upstream and downstream.

Table S2: Standard parameters for the peak identification algorithm which were chosen individually for each instrument.

Parameter	**Default**	**2B NO_x**	**2B NO_2**	**O_3**	**ICAD NO_x**	**ICAD NO_2**	**ICAD CO_2**	**Licor CO_2**	**BC**	**FMPS PNC**	**11-D PNC**	**EDM PNC**
Filter method[a]	**F, p, T**			-								
Typ. noise[b] [*x*] (1σ)		4	4	1	0.4	0.4	1	0.3	0.4			
Time resolution [s]		5	5	2	2–3	2–3	2	2–3	1	1	1	6
Window size[c] [min]	**10**											
Threshold interval[d] [s]	**30**											
Threshold factor[e] [σ]	**4**											
Max threshold[f] [*x*]		50	40	20	50	20	20	20	5	20 000	40	20
Points above thres[g] [s]	**3**											
Time below thres[h] [s]	**20**											
Mininum peak height [*x*]		50	20	10	50	10	10	10	2	10 000	20	20
Peak duration [s]:	**10–240**											
Offset between peak and ship passage[i] [s]:												
BRI	**-30 to 120**											
RIV	**-60 to 240**											

[a]Prior to analysis the raw instrument data was screened for flow rate (F), pressure (p) and temperature (T) conditions not in the range specified by the manufacturer. [b]Typical instrumental noise. *x* = unit depending on component, i.e. ppb for NO_x, NO_2 and O_3; ppm for CO_2; µg m^{-3} for BC; particles cm^3 for PNC. [c]Window size for background calculation (running median). [d]Interval length before peak start for calculation of the standard deviation to filter out periods with high atmospheric variability. [e]Number of standard deviations (σ) to determine the threshold for peak detection from the threshold interval. [f]Maximum permitted threshold value to filter out periods with increased atmospheric variability. [g]Minimum consecutive data points above the threshold to define the beginning of a peak. [h]Minimum time span below the threshold to define the end of a peak. [i]Temporal offset between the observed peak and the corresponding ship passage determined via AIS position (positive for peak occurring after ship passage).

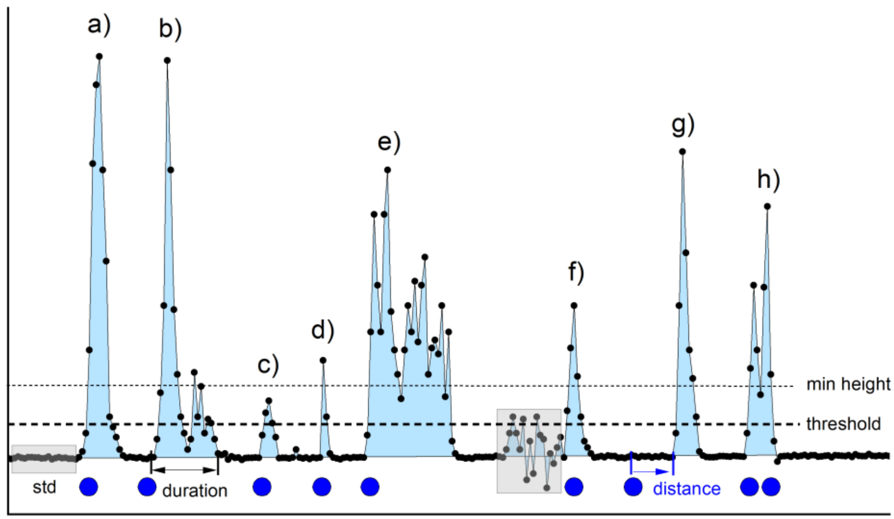

Figure S4: Exemplary peaks illustrating certain criteria of the peak identification algorithm according to Sect. 2.3.1 in the manuscript. A description of cases (a) to (h) is given in Table S2 below.

Table S3: Exemplary cases (a) to (h) belonging to Fig. S4.

Peak	**All criteria fullfilled**	peak > minimum height	3 points or more > threshold	peak duration < 4 min	low atmospheric background noise	distance between ship passage and deteced peak < 120 s	not more than 1 ship present within 120 s
a)	**yes**	yes	yes	yes	yes	yes	yes
b)	**yes**	yes	yes	yes	yes	yes	yes
c)	**no**	no	yes	yes	yes	yes	Yes
d)	**no**	yes	no	yes	yes	yes	Yes
e)	**no**	yes	yes	no	yes	yes	yes
f)	**no**	yes	yes	yes	no	yes	yes
g)	**no**	yes	yes	yes	yes	no	yes
h)	**no**	yes	yes	yes	yes	yes	no

Table S4: Emission factors (in g per kg fuel), NO_2-to-NO_x ratio (calculated for the initial time of emission), geometric mean diameter (GMD) and mode diameter (D_{mode}) for stations BRI and RIV.

BRI	NO_x	NO_2/NO_x (initial)	PM_1	BC	PNC (× 10^{15} #)	UFP (× 10^{15} #)	GMD (nm)	D_{mode} (nm)
Mean ± std	36.8 ± 15.7	0.08 ± 0.07	1.7 ± 1.1	0.5 ± 0.3	3.5 ± 5.5	3.2 ± 5.6	52 ± 23	66 ± 35
Median	33.8	0.07	1.6	0.4	1.5	1.0	55	81
25-75%	26.3 – 43.9	0.06 –0.09	0.9 – 2.3	0.3 – 0.7	1.0 – 3.3	0.7 – 2.9	31 – 70	26 – 93
IQR	17.6	0.03	1.4	0.4	2.3	2.2	39	67
min-max	1.5 – 184	0 – 1	0 – 13	0 – 3.8	0 – 92	0 – 92	8 – 114	6 – 143
N_{peaks}	3123	885	1780	1895	1780	1780	2010	2010
RIV	NO_x	NO_2/NO_x (initial)	$PM_{2.5}$	BC	$PN_{2.5}$ (× 10^{15})	PN_{UFP} (× 10^{15})	GMD (nm)	D_{mode} (nm)
Mean ± std	39.0 ± 15.7	-	-	-	-	-	-	-
Median	43.9	-	-	-	-	-	-	-
25-75%	29.4 – 47.6	-	-	-	-	-	-	-
IQR	18.2	-	-	-	-	-	-	-
min-max	8.7 – 81	-	-	-	-	-	-	-
N_{peaks}	47	-	-	-	-	-	-	-

Table S5: Ship classification scheme according to Krause et al. (2022) with emission factors derived in Krause et al. (2022) (converted with suggested fuel consumption scenario) together with E_{NOx} (in g kg^{-1}) and E_{PNC} (in particles kg^{-1}) measured at BRI.

Ship class	**length** [m]	**width** [m]	***N*** (this study)	$\boldsymbol{E_{NOx}}$ (this study) [g kg^{-1}]	***N*** (Krause et al.)	$\boldsymbol{E_{NOx}}$ (Krause et al.) [g kg^{-1}]	***N*** (this study)	$\boldsymbol{E_{PNC}}$ (this study) [10^{15} particles kg^{-1}]
All	-	-	3123	37 ± 16			1780	3.5 ± 5.5
I	≤ 39	≤ 6	13	36 ± 14	469	45 ± 3	8	4.9 ± 6.5
II	≤ 56	≤ 7	19	39 ± 21	49	44 ± 9	14	4.8 ± 5.9
III	≤ 68	≤ 9	27	42 ± 17	258	39 ± 3	9	10.9 ± 9.3
IV	≤ 86	≤ 10	330	40 ± 19	2608	47 ± 1	181	5.3 ± 7.2
Va	≤ 111	≤ 12	1550	36 ± 15	5377	50 ± 1	850	3.1 ± 4.2
Vb	≤ 136	≤ 12	412	36 ± 16	1548	49 ± 1	260	3.3 ± 5.7
Jowi	≤ 136	≤ 18	185	35 ± 14	1343	52 ± 2	110	3.9 ± 6.1
VIa	≤ 173	≤ 12	125	39 ± 16	285	57 ± 3	79	2.1 ± 2.2
VIb	≤ 194	≤ 23	408	37 ± 15	906	58 ± 2	243	3.7 ± 7.5
VIc	≤ 194	≤ 35	7	38 ± 11	280	47 ± 3	3	1.1 ± 0.9